

Search for the Rare Leptonic Decay $B^+ \rightarrow \mu^+ \nu_\mu$

B. Aubert,¹ R. Barate,¹ D. Boutigny,¹ F. Couderc,¹ J.-M. Gaillard,¹ A. Hicheur,¹ Y. Karyotakis,¹ J. P. Lees,¹ V. Tisserand,¹ A. Zghiche,¹ A. Palano,² A. Pompili,² J. C. Chen,³ N. D. Qi,³ G. Rong,³ P. Wang,³ Y. S. Zhu,³ G. Eigen,⁴ I. Ofte,⁴ B. Stugu,⁴ G. S. Abrams,⁵ A. W. Borgland,⁵ A. B. Breon,⁵ D. N. Brown,⁵ J. Button-Shafer,⁵ R. N. Cahn,⁵ E. Charles,⁵ C. T. Day,⁵ M. S. Gill,⁵ A. V. Gritsan,⁵ Y. Groysman,⁵ R. G. Jacobsen,⁵ R. W. Kadel,⁵ J. Kadyk,⁵ L. T. Kerth,⁵ Yu. G. Kolomensky,⁵ G. Kukartsev,⁵ C. LeClerc,⁵ M. E. Levi,⁵ G. Lynch,⁵ L. M. Mir,⁵ P. J. Oddone,⁵ T. J. Orimoto,⁵ M. Pripstein,⁵ N. A. Roe,⁵ M. T. Ronan,⁵ V. G. Shelkov,⁵ A. V. Telnov,⁵ W. A. Wenzel,⁵ K. Ford,⁶ T. J. Harrison,⁶ C. M. Hawkes,⁶ S. E. Morgan,⁶ A. T. Watson,⁶ N. K. Watson,⁶ M. Fritsch,⁷ K. Goetzen,⁷ T. Held,⁷ H. Koch,⁷ B. Lewandowski,⁷ M. Pelizaeus,⁷ K. Peters,⁷ H. Schmuecker,⁷ M. Steinke,⁷ J. T. Boyd,⁸ N. Chevalier,⁸ W. N. Cottingham,⁸ M. P. Kelly,⁸ T. E. Latham,⁸ C. Mackay,⁸ F. F. Wilson,⁸ K. Abe,⁹ T. Cuhadar-Donszelmann,⁹ C. Hearty,⁹ T. S. Mattison,⁹ J. A. McKenna,⁹ D. Thiessen,⁹ P. Kyberd,¹⁰ A. K. McKemey,¹⁰ L. Teodorescu,¹⁰ V. E. Blinov,¹¹ A. D. Bukin,¹¹ V. B. Golubev,¹¹ V. N. Ivanchenko,¹¹ E. A. Kravchenko,¹¹ A. P. Onuchin,¹¹ S. I. Serebnyakov,¹¹ Yu. I. Skovpen,¹¹ E. P. Solodov,¹¹ A. N. Yushkov,¹¹ D. Best,¹² M. Bruinsma,¹² M. Chao,¹² I. Eschrich,¹² D. Kirkby,¹² A. J. Lankford,¹² M. Mandelkern,¹² R. K. Mommsen,¹² W. Roethel,¹² D. P. Stoker,¹² C. Buchanan,¹³ B. L. Hartfiel,¹³ J. W. Gary,¹⁴ J. Layter,¹⁴ B. C. Shen,¹⁴ K. Wang,¹⁴ D. del Re,¹⁵ H. K. Hadavand,¹⁵ E. J. Hill,¹⁵ D. B. MacFarlane,¹⁵ H. P. Paar,¹⁵ Sh. Rahatlou,¹⁵ V. Sharma,¹⁵ J. W. Berryhill,¹⁶ C. Campagnari,¹⁶ B. Dahmes,¹⁶ S. L. Levy,¹⁶ O. Long,¹⁶ A. Lu,¹⁶ M. A. Mazur,¹⁶ J. D. Richman,¹⁶ W. Verkerke,¹⁶ T. W. Beck,¹⁷ J. Beringer,¹⁷ A. M. Eisner,¹⁷ C. A. Heusch,¹⁷ W. S. Lockman,¹⁷ T. Schalk,¹⁷ R. E. Schmitz,¹⁷ B. A. Schumm,¹⁷ A. Seiden,¹⁷ P. Spradlin,¹⁷ W. Walkowiak,¹⁷ D. C. Williams,¹⁷ M. G. Wilson,¹⁷ J. Albert,¹⁸ E. Chen,¹⁸ G. P. Dubois-Felsmann,¹⁸ A. Dvoretzskii,¹⁸ R. J. Erwin,¹⁸ D. G. Hitlin,¹⁸ I. Narsky,¹⁸ T. Piatenko,¹⁸ F. C. Porter,¹⁸ A. Ryd,¹⁸ A. Samuel,¹⁸ S. Yang,¹⁸ S. Jayatilleke,¹⁹ G. Mancinelli,¹⁹ B. T. Meadows,¹⁹ M. D. Sokoloff,¹⁹ T. Abe,²⁰ F. Blanc,²⁰ P. Bloom,²⁰ S. Chen,²⁰ P. J. Clark,²⁰ W. T. Ford,²⁰ U. Nauenberg,²⁰ A. Olivas,²⁰ P. Rankin,²⁰ J. Roy,²⁰ J. G. Smith,²⁰ W. C. van Hoek,²⁰ L. Zhang,²⁰ J. L. Harton,²¹ T. Hu,²¹ A. Soffer,²¹ W. H. Toki,²¹ R. J. Wilson,²¹ J. Zhang,²¹ D. Altenburg,²² T. Brandt,²² J. Brose,²² T. Colberg,²² M. Dickopp,²² E. Feltresi,²² A. Hauke,²² H. M. Lacker,²² E. Maly,²² R. Müller-Pfefferkorn,²² R. Nogowski,²² S. Otto,²² J. Schubert,²² K. R. Schubert,²² R. Schwierz,²² B. Spaan,²² D. Bernard,²³ G. R. Bonneaud,²³ F. Brochard,²³ P. Grenier,²³ Ch. Thiebaut,²³ G. Vasileiadis,²³ M. Verderi,²³ D. J. Bard,²⁴ A. Khan,²⁴ D. Lavin,²⁴ F. Muheim,²⁴ S. Playfer,²⁴ M. Andreotti,²⁵ V. Azzolini,²⁵ D. Bettoni,²⁵ C. Bozzi,²⁵ R. Calabrese,²⁵ G. Cibinetto,²⁵ E. Luppi,²⁵ M. Negrini,²⁵ L. Piemontese,²⁵ A. Sarti,²⁵ E. Treadwell,²⁶ R. Baldini-Ferroli,²⁷ A. Calcaterra,²⁷ R. de Sangro,²⁷ G. Finocchiaro,²⁷ P. Patteri,²⁷ M. Piccolo,²⁷ A. Zallo,²⁷ A. Buzzo,²⁸ R. Capra,²⁸ R. Contri,²⁸ G. Crosetti,²⁸ M. Lo Vetere,²⁸ M. Macri,²⁸ M. R. Monge,²⁸ S. Passaggio,²⁸ C. Patrignani,²⁸ E. Robutti,²⁸ A. Santroni,²⁸ S. Tosi,²⁸ S. Bailey,²⁹ M. Morii,²⁹ E. Won,²⁹ R. S. Dubitzky,³⁰ U. Langenegger,³⁰ W. Bhimji,³¹ D. A. Bowerman,³¹ P. D. Dauncey,³¹ U. Egede,³¹ J. R. Gaillard,³¹ G. W. Morton,³¹ J. A. Nash,³¹ G. P. Taylor,³¹ G. J. Grenier,³² S.-J. Lee,³² U. Mallik,³² J. Cochran,³³ H. B. Crawley,³³ J. Lamsa,³³ W. T. Meyer,³³ S. Prell,³³ E. I. Rosenberg,³³ J. Yi,³³ M. Davier,³⁴ G. Grosdidier,³⁴ A. Höcker,³⁴ S. Laplace,³⁴ F. Le Diberder,³⁴ V. Lepeltier,³⁴ A. M. Lutz,³⁴ T. C. Petersen,³⁴ S. Plaszczynski,³⁴ M. H. Schune,³⁴ L. Tantot,³⁴ G. Wormser,³⁴ V. Brigljević,³⁵ C. H. Cheng,³⁵ D. J. Lange,³⁵ M. C. Simani,³⁵ D. M. Wright,³⁵ A. J. Bevan,³⁶ J. P. Coleman,³⁶ J. R. Fry,³⁶ E. Gabathuler,³⁶ R. Gamet,³⁶ M. Kay,³⁶ R. J. Parry,³⁶ D. J. Payne,³⁶ R. J. Sloane,³⁶ C. Touramanis,³⁶ J. J. Back,³⁷ P. F. Harrison,³⁷ G. B. Mohanty,³⁷ C. L. Brown,³⁸ G. Cowan,³⁸ R. L. Flack,³⁸ H. U. Flaecher,³⁸ S. George,³⁸ M. G. Green,³⁸ A. Kurup,³⁸ C. E. Marker,³⁸ T. R. McMahon,³⁸ S. Ricciardi,³⁸ F. Salvatore,³⁸ G. Vaitsas,³⁸ M. A. Winter,³⁸ D. Brown,³⁹ C. L. Davis,³⁹ J. Allison,⁴⁰ N. R. Barlow,⁴⁰ R. J. Barlow,⁴⁰ P. A. Hart,⁴⁰ M. C. Hodgkinson,⁴⁰ G. D. Lafferty,⁴⁰ A. J. Lyon,⁴⁰ J. C. Williams,⁴⁰ A. Farbin,⁴¹ W. D. Hulsbergen,⁴¹ A. Jawahery,⁴¹ D. Kovalskyi,⁴¹ C. K. Lae,⁴¹ V. Lillard,⁴¹ D. A. Roberts,⁴¹ G. Blaylock,⁴² C. Dallapiccola,⁴² K. T. Flood,⁴² S. S. Hertzbach,⁴² R. Kofler,⁴² V. B. Koptchev,⁴² T. B. Moore,⁴² S. Saremi,⁴² H. Staengle,⁴² S. Willocq,⁴² R. Cowan,⁴³ G. Sciolla,⁴³ F. Taylor,⁴³ R. K. Yamamoto,⁴³ D. J. J. Mangeol,⁴⁴ P. M. Patel,⁴⁴ S. H. Robertson,⁴⁴ A. Lazzaro,⁴⁵ F. Palombo,⁴⁵ J. M. Bauer,⁴⁶ L. Cremaldi,⁴⁶ V. Eschenburg,⁴⁶ R. Godang,⁴⁶ R. Kroeger,⁴⁶ J. Reidy,⁴⁶ D. A. Sanders,⁴⁶ D. J. Summers,⁴⁶ H. W. Zhao,⁴⁶ S. Brunet,⁴⁷ D. Cote-Ahern,⁴⁷ P. Taras,⁴⁷ H. Nicholson,⁴⁸ C. Cartaro,⁴⁹ N. Cavallo,⁴⁹ G. De Nardo,⁴⁹ F. Fabozzi,^{49,*} C. Gatto,⁴⁹ L. Lista,⁴⁹ P. Paolucci,⁴⁹ D. Piccolo,⁴⁹ C. Sciacca,⁴⁹ M. A. Baak,⁵⁰ G. Raven,⁵⁰ L. Wilden,⁵⁰ C. P. Jessop,⁵¹ J. M. LoSecco,⁵¹ T. A. Gabriel,⁵² T. Allmendinger,⁵³ B. Brau,⁵³ K. K. Gan,⁵³ K. Honscheid,⁵³ D. Hufnagel,⁵³ H. Kagan,⁵³ R. Kass,⁵³ T. Pulliam,⁵³ R. Ter-Antonyan,⁵³ Q. K. Wong,⁵³ J. Brau,⁵⁴ R. Frey,⁵⁴ O. Igonkina,⁵⁴ C. T. Potter,⁵⁴ N. B. Sinev,⁵⁴ D. Strom,⁵⁴

E. Torrence,⁵⁴ F. Colecchia,⁵⁵ A. Dorigo,⁵⁵ F. Galeazzi,⁵⁵ M. Margoni,⁵⁵ M. Morandin,⁵⁵ M. Posocco,⁵⁵ M. Rotondo,⁵⁵ F. Simonetto,⁵⁵ R. Stroili,⁵⁵ G. Tiozzo,⁵⁵ C. Voci,⁵⁵ M. Benayoun,⁵⁶ H. Briand,⁵⁶ J. Chauveau,⁵⁶ P. David,⁵⁶ Ch. de la Vaissière,⁵⁶ L. Del Buono,⁵⁶ O. Hamon,⁵⁶ M. J. J. John,⁵⁶ Ph. Leruste,⁵⁶ J. Ocariz,⁵⁶ M. Pivk,⁵⁶ L. Roos,⁵⁶ S. T'Jampens,⁵⁶ G. Therin,⁵⁶ P. F. Manfredi,⁵⁷ V. Re,⁵⁷ P. K. Behera,⁵⁸ L. Gladney,⁵⁸ Q. H. Guo,⁵⁸ J. Panetta,⁵⁸ F. Anulli,^{27,59} M. Biasini,⁵⁹ I. M. Peruzzi,^{27,59} M. Pioppi,⁵⁹ C. Angelini,⁶⁰ G. Batignani,⁶⁰ S. Bettarini,⁶⁰ M. Bondioli,⁶⁰ F. Bucci,⁶⁰ G. Calderini,⁶⁰ M. Carpinelli,⁶⁰ V. Del Gamba,⁶⁰ F. Forti,⁶⁰ M. A. Giorgi,⁶⁰ A. Lusiani,⁶⁰ G. Marchiori,⁶⁰ F. Martinez-Vidal,^{60,†} M. Morganti,⁶⁰ N. Neri,⁶⁰ E. Paoloni,⁶⁰ M. Rama,⁶⁰ G. Rizzo,⁶⁰ F. Sandrelli,⁶⁰ J. Walsh,⁶⁰ M. Haire,⁶¹ D. Judd,⁶¹ K. Paick,⁶¹ D. E. Wagoner,⁶¹ N. Danielson,⁶² P. Elmer,⁶² C. Lu,⁶² V. Miftakov,⁶² J. Olsen,⁶² A. J. S. Smith,⁶² E. W. Varnes,⁶² F. Bellini,⁶³ G. Cavoto,^{62,63} R. Faccini,⁶³ F. Ferrarotto,⁶³ F. Ferroni,⁶³ M. Gaspero,⁶³ M. A. Mazzone,⁶³ S. Morganti,⁶³ M. Pierini,⁶³ G. Piredda,⁶³ F. Safai Tehrani,⁶³ C. Voena,⁶³ S. Christ,⁶⁴ G. Wagner,⁶⁴ R. Waldi,⁶⁴ T. Adye,⁶⁵ N. De Groot,⁶⁵ B. Franek,⁶⁵ N. I. Geddes,⁶⁵ G. P. Gopal,⁶⁵ E. O. Olaiya,⁶⁵ S. M. Xella,⁶⁵ R. Aleksan,⁶⁶ S. Emery,⁶⁶ A. Gaidot,⁶⁶ S. F. Ganzhur,⁶⁶ P.-F. Giraud,⁶⁶ G. Hamel de Monchenault,⁶⁶ W. Kozanecki,⁶⁶ M. Langer,⁶⁶ M. Legendre,⁶⁶ G. W. London,⁶⁶ B. Mayer,⁶⁶ G. Schott,⁶⁶ G. Vasseur,⁶⁶ Ch. Yeche,⁶⁶ M. Zito,⁶⁶ M. V. Purohit,⁶⁷ A. W. Weidemann,⁶⁷ F. X. Yumiceva,⁶⁷ D. Aston,⁶⁸ R. Bartoldus,⁶⁸ N. Berger,⁶⁸ A. M. Boyarski,⁶⁸ O. L. Buchmueller,⁶⁸ M. R. Convery,⁶⁸ M. Cristinziani,⁶⁸ D. Dong,⁶⁸ J. Dorfan,⁶⁸ D. Dujmic,⁶⁸ W. Dunwoodie,⁶⁸ E. E. Elsen,⁶⁸ R. C. Field,⁶⁸ T. Glanzman,⁶⁸ S. J. Gowdy,⁶⁸ T. Hadig,⁶⁸ V. Halyo,⁶⁸ T. Hryn'ova,⁶⁸ W. R. Innes,⁶⁸ M. H. Kelsey,⁶⁸ P. Kim,⁶⁸ M. L. Kocian,⁶⁸ D. W. G. S. Leith,⁶⁸ J. Libby,⁶⁸ S. Luitz,⁶⁸ V. Luth,⁶⁸ H. L. Lynch,⁶⁸ H. Marsiske,⁶⁸ R. Messner,⁶⁸ D. R. Muller,⁶⁸ C. P. O'Grady,⁶⁸ V. E. Ozcan,⁶⁸ A. Perazzo,⁶⁸ M. Perl,⁶⁸ S. Petrak,⁶⁸ B. N. Ratcliff,⁶⁸ A. Roodman,⁶⁸ A. A. Salnikov,⁶⁸ R. H. Schindler,⁶⁸ J. Schwiening,⁶⁸ G. Simi,⁶⁸ A. Snyder,⁶⁸ A. Soha,⁶⁸ J. Stelzer,⁶⁸ D. Su,⁶⁸ M. K. Sullivan,⁶⁸ J. Va'vra,⁶⁸ S. R. Wagner,⁶⁸ M. Weaver,⁶⁸ A. J. R. Weinstein,⁶⁸ W. J. Wisniewski,⁶⁸ D. H. Wright,⁶⁸ C. C. Young,⁶⁸ P. R. Burchat,⁶⁹ A. J. Edwards,⁶⁹ T. I. Meyer,⁶⁹ B. A. Petersen,⁶⁹ C. Roat,⁶⁹ M. Ahmed,⁷⁰ S. Ahmed,⁷⁰ M. S. Alam,⁷⁰ J. A. Ernst,⁷⁰ M. A. Saeed,⁷⁰ M. Saleem,⁷⁰ F. R. Wappler,⁷⁰ W. Bugg,⁷¹ M. Krishnamurthy,⁷¹ S. M. Spanier,⁷¹ R. Eckmann,⁷² H. Kim,⁷² J. L. Ritchie,⁷² A. Satpathy,⁷² R. F. Schwitters,⁷² J. M. Izen,⁷³ I. Kitayama,⁷³ X. C. Lou,⁷³ S. Ye,⁷³ F. Bianchi,⁷⁴ M. Bona,⁷⁴ F. Gallo,⁷⁴ D. Gamba,⁷⁴ C. Borean,⁷⁵ L. Bosisio,⁷⁵ F. Cossutti,⁷⁵ G. Della Ricca,⁷⁵ S. Dittongo,⁷⁵ S. Grancagnolo,⁷⁵ L. Lanceri,⁷⁵ P. Poropat,^{75,‡} L. Vitale,⁷⁵ G. Vuagnin,⁷⁵ R. S. Panvini,⁷⁶ Sw. Banerjee,⁷⁷ C. M. Brown,⁷⁷ D. Fortin,⁷⁷ P. D. Jackson,⁷⁷ R. Kowalewski,⁷⁷ J. M. Roney,⁷⁷ H. R. Band,⁷⁸ S. Dasu,⁷⁸ M. Datta,⁷⁸ A. M. Eichenbaum,⁷⁸ J. R. Johnson,⁷⁸ P. E. Kutter,⁷⁸ H. Li,⁷⁸ R. Liu,⁷⁸ F. Di Lodovico,⁷⁸ A. Mihalyi,⁷⁸ A. K. Mohapatra,⁷⁸ Y. Pan,⁷⁸ R. Prepost,⁷⁸ S. J. Sekula,⁷⁸ J. H. von Wimmersperg-Toeller,⁷⁸ J. Wu,⁷⁸ S. L. Wu,⁷⁸ Z. Yu,⁷⁸ and H. Neal⁷⁹

(BABAR Collaboration)

¹Laboratoire de Physique des Particules, F-74941 Annecy-le-Vieux, France

²Dipartimento di Fisica and INFN, Università di Bari, I-70126 Bari, Italy

³Institute of High Energy Physics, Beijing 100039, China

⁴Institute of Physics, University of Bergen, N-5007 Bergen, Norway

⁵Lawrence Berkeley National Laboratory and University of California, Berkeley, California 94720, USA

⁶University of Birmingham, Birmingham, B15 2TT, United Kingdom

⁷Institut für Experimentalphysik I, Ruhr Universität Bochum, D-44780 Bochum, Germany

⁸University of Bristol, Bristol BS8 1TL, United Kingdom

⁹University of British Columbia, Vancouver, British Columbia, Canada V6T 1Z1

¹⁰Brunel University, Uxbridge, Middlesex UB8 3PH, United Kingdom

¹¹Budker Institute of Nuclear Physics, Novosibirsk 630090, Russia

¹²University of California at Irvine, Irvine, California 92697, USA

¹³University of California at Los Angeles, Los Angeles, California 90024, USA

¹⁴University of California at Riverside, Riverside, California 92521, USA

¹⁵University of California at San Diego, La Jolla, California 92093, USA

¹⁶University of California at Santa Barbara, Santa Barbara, California 93106, USA

¹⁷Institute for Particle Physics, University of California at Santa Cruz, Santa Cruz, California 95064, USA

¹⁸California Institute of Technology, Pasadena, California 91125, USA

¹⁹University of Cincinnati, Cincinnati, Ohio 45221, USA

²⁰University of Colorado, Boulder, Colorado 80309, USA

²¹Colorado State University, Fort Collins, Colorado 80523, USA

- ²²*Institut für Kern- und Teilchenphysik, Technische Universität Dresden, D-01062 Dresden, Germany*
²³*Ecole Polytechnique, LLR, F-91128 Palaiseau, France*
²⁴*University of Edinburgh, Edinburgh EH9 3JZ, United Kingdom*
²⁵*Dipartimento di Fisica and INFN, Università di Ferrara, I-44100 Ferrara, Italy*
²⁶*Florida A&M University, Tallahassee, Florida 32307, USA*
²⁷*Laboratori Nazionali di Frascati dell'INFN, I-00044 Frascati, Italy*
²⁸*Dipartimento di Fisica and INFN, Università di Genova, I-16146 Genova, Italy*
²⁹*Harvard University, Cambridge, Massachusetts 02138, USA*
³⁰*Physikalisches Institut, Universität Heidelberg, Philosophenweg 12, D-69120 Heidelberg, Germany*
³¹*Imperial College London, London, SW7 2BW, United Kingdom*
³²*University of Iowa, Iowa City, Iowa 52242, USA*
³³*Iowa State University, Ames, Iowa 50011-3160, USA*
³⁴*Laboratoire de l'Accélérateur Linéaire, F-91898 Orsay, France*
³⁵*Lawrence Livermore National Laboratory, Livermore, California 94550, USA*
³⁶*University of Liverpool, Liverpool L69 3BX, United Kingdom*
³⁷*Queen Mary, University of London, E1 4NS, United Kingdom*
³⁸*Royal Holloway and Bedford New College, University of London, Egham, Surrey TW20 0EX, United Kingdom*
³⁹*University of Louisville, Louisville, Kentucky 40292, USA*
⁴⁰*University of Manchester, Manchester M13 9PL, United Kingdom*
⁴¹*University of Maryland, College Park, Maryland 20742, USA*
⁴²*University of Massachusetts, Amherst, Massachusetts 01003, USA*
⁴³*Laboratory for Nuclear Science, Massachusetts Institute of Technology, Cambridge, Massachusetts 02139, USA*
⁴⁴*McGill University, Montréal, Quebec, Canada H3A 2T8*
⁴⁵*Dipartimento di Fisica and INFN, Università di Milano, I-20133 Milano, Italy*
⁴⁶*University of Mississippi, University, Mississippi 38677, USA*
⁴⁷*Laboratoire René J. A. Lévesque, Université de Montréal, Montréal, Quebec, Canada H3C 3J7*
⁴⁸*Mount Holyoke College, South Hadley, Massachusetts 01075, USA*
⁴⁹*Dipartimento di Scienze Fisiche and INFN, Università di Napoli Federico II, I-80126, Napoli, Italy*
⁵⁰*National Institute for Nuclear Physics and High Energy Physics, NIKHEF, NL-1009 DB Amsterdam, The Netherlands*
⁵¹*University of Notre Dame, Notre Dame, Indiana 46556, USA*
⁵²*Oak Ridge National Laboratory, Oak Ridge, Tennessee 37831, USA*
⁵³*The Ohio State University, Columbus, Ohio 43210, USA*
⁵⁴*University of Oregon, Eugene, Oregon 97403, USA*
⁵⁵*Dipartimento di Fisica and INFN, Università di Padova, I-35131 Padova, Italy*
⁵⁶*Lab de Physique Nucléaire H. E., Universités Paris VI et VII, F-75252 Paris, France*
⁵⁷*Dipartimento di Elettronica and INFN, Università di Pavia, I-27100 Pavia, Italy*
⁵⁸*University of Pennsylvania, Philadelphia, Pennsylvania 19104, USA*
⁵⁹*Dipartimento di Fisica and INFN, Università di Perugia, I-06100 Perugia, Italy*
⁶⁰*Dipartimento di Fisica, Scuola Normale Superiore and INFN, Università di Pisa, I-56127 Pisa, Italy*
⁶¹*Prairie View A&M University, Prairie View, Texas 77446, USA*
⁶²*Princeton University, Princeton, New Jersey 08544, USA*
⁶³*Dipartimento di Fisica and INFN, Università di Roma La Sapienza, I-00185 Roma, Italy*
⁶⁴*Universität Rostock, D-18051 Rostock, Germany*
⁶⁵*Rutherford Appleton Laboratory, Chilton, Didcot, Oxon, OX11 0QX, United Kingdom*
⁶⁶*CEA/Saclay, DSM/Dapnia, F-91191 Gif-sur-Yvette, France*
⁶⁷*University of South Carolina, Columbia, South Carolina 29208, USA*
⁶⁸*Stanford Linear Accelerator Center, Stanford, California 94309, USA*
⁶⁹*Stanford University, Stanford, California 94305-4060, USA*
⁷⁰*State University of New York, Albany, New York 12222, USA*
⁷¹*University of Tennessee, Knoxville, Tennessee 37996, USA*
⁷²*University of Texas at Austin, Austin, Texas 78712, USA*
⁷³*University of Texas at Dallas, Richardson, Texas 75083, USA*
⁷⁴*Dipartimento di Fisica Sperimentale and INFN, Università di Torino, I-10125 Torino, Italy*
⁷⁵*Dipartimento di Fisica and INFN, Università di Trieste, I-34127 Trieste, Italy*
⁷⁶*Vanderbilt University, Nashville, Tennessee 37235, USA*
⁷⁷*University of Victoria, Victoria, British Columbia, Canada V8W 3P6*
⁷⁸*University of Wisconsin, Madison, Wisconsin 53706, USA*
⁷⁹*Yale University, New Haven, Connecticut 06511, USA*

(Received 5 January 2004; published 3 June 2004; publisher error corrected 14 October 2004)

We have performed a search for the rare leptonic decay $B^+ \rightarrow \mu^+ \nu_\mu$ with data collected at the $Y(4S)$ resonance by the *BABAR* experiment at the PEP-II storage ring. In a sample of $88.4 \times 10^6 B\bar{B}$ pairs, we find no significant evidence for a signal and set an upper limit on the branching fraction $\mathcal{B}(B^+ \rightarrow \mu^+ \nu_\mu) < 6.6 \times 10^{-6}$ at the 90% confidence level.

DOI: 10.1103/PhysRevLett.92.221803

PACS numbers: 13.25.Hw, 11.30.Er, 12.15.Hh

The study of the purely leptonic decays $B^+ \rightarrow \ell^+ \nu_\ell$ ($\ell = e, \mu, \text{ or } \tau$) can provide sensitivity to poorly constrained standard model (SM) parameters and also act as a probe of new physics. In the SM, these decays proceed by annihilation to a W boson with a branching fraction given by

$$\mathcal{B}(B^+ \rightarrow \ell^+ \nu_\ell) = \frac{G_F^2 m_B m_\ell^2}{8\pi} \left(1 - \frac{m_\ell^2}{m_B^2}\right)^2 f_B^2 |V_{ub}|^2 \tau_{B^+},$$

where G_F is the Fermi coupling constant, m_ℓ and m_B are the lepton and B meson masses, and τ_{B^+} is the B^+ lifetime. The decay rate is sensitive to the product of the Cabibbo-Kobayashi-Maskawa matrix element $|V_{ub}|$ and the B decay constant f_B , which is proportional to the wave function for zero separation between the quarks. Currently, our best understanding of f_B comes from lattice gauge calculations where the theoretical uncertainty is roughly 15% [1]. This uncertainty is a significant limitation on the extraction of $|V_{ud}|$ from precision $B^0\bar{B}^0$ mixing measurements [1]. Observation of $B^+ \rightarrow \ell^+ \nu_\ell$ could provide the first direct measurement of f_B .

In this Letter, we present a search for the decay $B^+ \rightarrow \mu^+ \nu_\mu$ (charge conjugation is implied throughout this paper). This decay is highly suppressed due to the dependence on $|V_{ub}|^2$ and m_ℓ^2 (helicity suppression). The SM prediction for the $B^+ \rightarrow \mu^+ \nu_\mu$ branching fraction is roughly $(2\text{--}6) \times 10^{-7}$ while the current best published limit is $\mathcal{B}(B^+ \rightarrow \mu^+ \nu_\mu) < 2.1 \times 10^{-5}$ at the 90% C.L. [2]. Although the expected branching fraction for $B^+ \rightarrow \tau^+ \nu_\tau$ is larger by a factor of 225 due to the increased lepton mass, the additional neutrinos produced in the tau decay make the search more challenging experimentally. The current best limit is $\mathcal{B}(B^+ \rightarrow \tau^+ \nu_\tau) < 5.7 \times 10^{-4}$ [3].

The $B^+ \rightarrow \ell^+ \nu_\ell$ decay modes are also potentially sensitive to physics beyond the SM. For example, in two-Higgs-doublet models such as the minimal supersymmetric standard model (MSSM), these decays can proceed at tree level via an intermediate H^\pm , providing a possible enhancement up to current experimental limits [4]. Similarly, in R -parity violating extensions of the MSSM, $B^+ \rightarrow \ell^+ \nu_\ell$ may be mediated by scalar supersymmetric particles [5]. Hence, upper limits on the $B^+ \rightarrow \ell^+ \nu_\ell$ branching fractions constrain the R -parity violating couplings.

The data used in this analysis were collected with the *BABAR* detector at the PEP-II storage ring. The data sample consists of an integrated luminosity of 81.4 fb^{-1}

accumulated at the $Y(4S)$ resonance (“on-resonance”) and 9.6 fb^{-1} accumulated at a center-of-mass (C.M.) energy about 40 MeV below the $Y(4S)$ resonance (“off-resonance”). The on-resonance sample corresponds to $88.4 \times 10^6 B\bar{B}$ pairs.

The *BABAR* detector is optimized for the asymmetric collisions at PEP-II and is described in detail elsewhere [6]. Charged particle trajectories are measured with a five-layer double-sided silicon vertex tracker (SVT) and a 40-layer drift chamber (DCH), which are contained in the 1.5 T magnetic field of a superconducting solenoid. A detector of internally reflected Cherenkov radiation provides identification of charged kaons and pions. The energies of neutral particles are measured by an electromagnetic calorimeter (EMC) consisting of 6580 CsI(Tl) crystals. The flux return of the solenoid is instrumented with resistive plate chambers to provide muon identification (IFR). A Monte Carlo (MC) simulation of the *BABAR* detector based on GEANT4 [7] was used to optimize the signal selection criteria and evaluate the signal efficiency.

The $B^+ \rightarrow \mu^+ \nu_\mu$ decay produces a monoenergetic muon in the B rest frame with $p_\mu \approx m_B/2$. Since the neutrino goes undetected, we assume that all remaining particles are associated with the decay of the other B in the event, which we denote the “companion” B . Signal events are selected using the kinematic variables $\Delta E = E_B^* - E_b^*$ and energy-substituted mass, $m_{ES} = \sqrt{E_b^{*2} - \mathbf{p}_B^{*2}}$, where \mathbf{p}_B^* (E_B^*) is the momentum (energy) of the reconstructed companion B and E_b^* is the beam energy, all in the $Y(4S)$ rest frame. We require m_{ES} to be consistent with the B meson mass, and the energy of the companion B to be consistent with E_b^* resulting in $\Delta E \simeq 0$.

To reduce nonhadronic backgrounds, we select events that contain at least four charged tracks and have a normalized second Fox-Wolfram moment [8] less than 0.98. Muon candidates are required to penetrate at least 2.2 interaction lengths of material in the IFR, have a measured penetration within 0.8 interaction lengths of that expected for a muon, and have an associated energy in the EMC consistent with that of a minimum-ionizing particle. The muon track must have at least 12 DCH hits, momentum transverse to the beam axis $p_\perp > 0.1 \text{ GeV}/c$, and a point of closest approach to the interaction point that is within 10 cm along the beam axis and less than 1.5 cm in the transverse plane. For each muon candidate with momentum between 2.25 and 2.95 GeV/c

in the C.M. frame, we attempt to reconstruct the companion B .

The companion B is formed from all charged tracks satisfying the above criteria regarding the distance of closest approach to the interaction point. It also includes all calorimeter clusters with energy greater than 30 MeV that are not associated with a charged track. Particle identification is applied to the charged tracks to identify electrons, muons, kaons, and protons while the remaining unidentified tracks are assumed to be pions. The resulting mass hypotheses are applied to improve the ΔE resolution. Events with additional identified leptons are discarded since they typically arise from semileptonic B or charm decays and indicate the presence of additional neutrinos.

Once the companion B is reconstructed, we calculate the muon momentum in the rest frame of the signal B . We assume the signal B travels in the direction opposite to that of the companion B momentum in the $Y(4S)$ rest frame with a momentum determined by the two-body decay $Y(4S) \rightarrow B^+ B^-$. For signal muons, the p_μ distribution peaks at 2.64 GeV/ c with an rms of about 100 MeV/ c .

The two most significant backgrounds are B semileptonic decays involving $b \rightarrow u\mu\bar{\nu}$ transitions where the end point of the muon spectrum approaches that of the signal, and nonresonant $q\bar{q}$ (“continuum”) events where a charged pion is mistakenly identified as a muon. Using a pion control sample obtained from $e^+e^- \rightarrow \tau^+\tau^-$ events in the data, the misidentification probability is estimated to be 2% in the momentum and polar angle region relevant for $B^+ \rightarrow \mu^+\nu_\mu$. The muon candidate momentum spectrum of the background decreases with increasing momentum so we apply an asymmetric cut about the signal peak, $2.58 < p_\mu < 2.78$ GeV/ c .

In order for continuum events to populate the signal region of ΔE and m_{ES} , there must be significant missing energy due to particles outside the detector acceptance, unreconstructed neutral hadrons, or additional neutrinos. Therefore, we require $|\cos\theta_\nu| < 0.88$ so that the polar angle of the missing momentum vector in the laboratory frame, θ_ν , is directed into the detector’s fiducial volume. Furthermore, these events tend to produce a jetlike event topology, whereas $B\bar{B}$ events tend to be spherical. We define a variable, θ_T^* , which is the angle between the muon candidate momentum and the thrust axis of the companion B in the C.M. frame. By requiring $|\cos\theta_T^*| < 0.55$, we remove approximately 98% of the continuum background while retaining 54% of the signal decays.

We select $B^+ \rightarrow \mu^+\nu_\mu$ signal candidates with simultaneous requirements on ΔE and m_{ES} , thus forming a “signal box” defined by $-0.75 < \Delta E < 0.5$ GeV and $m_{ES} > 5.27$ GeV/ c^2 . The dimensions of the signal box, as well as the above requirements on p_μ , $|\cos\theta_T^*|$, and $|\cos\theta_\nu|$, were determined using an optimization procedure that finds the combination of cuts that maximizes the

TABLE I. The boundaries of the signal box and various sidebands defined for this analysis.

Region	ΔE (GeV)	m_{ES} (GeV/ c^2)
Signal box	[−0.75, 0.50]	>5.27
Blinding box	[−1.30, 0.70]	>5.24
Fit sideband	[−0.75, 0.50]	[5.10, 5.24]
ΔE sideband (bottom)	[−3.00, −1.30]	>5.10
ΔE sideband (top)	[0.70, 1.50]	>5.10

quantity $S/\sqrt{S+B}$, where S and B are the signal and background yields in the MC simulation, respectively. The signal branching fraction was set to the SM expectation during the optimization procedure. After applying all selection criteria, the $B^+ \rightarrow \mu^+\nu_\mu$ efficiency is determined from the simulation to be $(2.24 \pm 0.07)\%$.

In addition to the signal box, we have defined a slightly larger blinding box and three sideband regions. The boundaries of these regions in the $(\Delta E, m_{ES})$ plane are listed in Table I. The data within the blinding box were kept hidden until the analysis was completed in order to avoid the introduction of bias in the event-selection process.

We estimate the background in the signal box assuming that the m_{ES} distribution is described by the ARGUS function [9]. This assumption is consistent with the observed distributions in the MC simulation as well as the data in the ΔE sidebands. The shape parameter of the ARGUS function (ζ) is determined from an unbinned maximum likelihood fit using the data in the fit sideband defined in Table I. The ARGUS shape (A) is extrapolated through the signal box and constrained to be zero at the end point, which is fixed at $E_b^* = 5.29$ GeV/ c^2 . Figure 1 shows the results of the fit. The expected background is

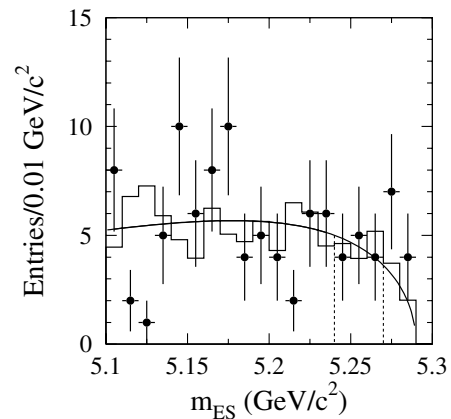


FIG. 1. Results of the ARGUS fit to the on-resonance data satisfying $-0.75 < \Delta E < 0.5$ GeV. The two dashed lines indicate the lower boundaries of the blinded region and signal box at 5.24 and 5.27 GeV/ c^2 , respectively. The histogram shows the sum of all simulated background sources normalized to the on-resonance luminosity.

calculated using

$$N_{\text{bkg}} = N_{\text{fit}} \times \frac{\int_{5.27}^{5.29} A(m_{\text{ES}}) dm_{\text{ES}}}{\int_{5.10}^{5.24} A(m_{\text{ES}}) dm_{\text{ES}}} \equiv N_{\text{fit}} \times R_{\text{ARGUS}}, \quad (1)$$

where N_{fit} is the number of events contributing to the fit. The result is $N_{\text{bkg}} = 5.0^{+1.8}_{-1.4}$ events. The uncertainty is determined by varying ζ by the $\pm 1\sigma$ uncertainty from the fit. In the MC simulation (scaled to the on-resonance luminosity), we find 5.7 ± 0.5 background events in the signal box, in agreement with the data extrapolation. The simulation indicates that the background is primarily continuum, consisting of 57% light-quark ($u\bar{u}$, $d\bar{d}$, $s\bar{s}$), 23% $c\bar{c}$, and 20% $B\bar{B}$ events.

By using the ARGUS function to describe the background m_{ES} distribution, we would underestimate the contribution of backgrounds that peak within the blinded region. The simulation indicates that only the relatively small component of background from $B\bar{B}$ events exhibits a mildly peaking m_{ES} distribution. When the background extrapolation is applied to the simulation, the resulting background estimate is 5.2 ± 0.5 events, in agreement with the 5.7 events actually found in the signal box. Although neglecting peaking backgrounds could enhance an apparent signal, here the result would be a more conservative upper limit.

We have evaluated the systematic uncertainty in the signal efficiency which includes the muon candidate selection as well as the reconstruction efficiency of the companion B . Using a muon control sample obtained from $e^+e^- \rightarrow e^+e^-\mu^+\mu^-$ events in the data, the muon identification efficiency has been measured in bins of momentum, polar angle, and charge, and the results are incorporated into the nominal MC simulation. Averaged over the momentum and polar angle distributions of muons from $B^+ \rightarrow \mu^+\nu_\mu$, we estimate that the muon identification efficiency for this data sample is 61% with a systematic uncertainty of 4.2%. From the fraction of tracks reconstructed in the SVT that are also found in the DCH, we find that the tracking efficiency of the muon candidate is overestimated in the simulation by 0.8%, which is applied as a correction to the signal efficiency. The associated systematic error is 2%. An additional systematic error of 1% is included due to the requirement that the event contain at least four charged tracks.

The companion B reconstruction efficiency has been studied using a control sample of fully reconstructed $B^+ \rightarrow D^{(*)0}\pi^+$ events. These are also two-body decays in which the π^+ momentum spectrum is similar to that of the μ^+ in signal events. Once reconstructed, the pion can be treated as if it were the signal muon and the $D^{(*)0}$ decay products can be removed from the event to simulate the unobserved neutrino. Then the companion B is reconstructed in the control sample as it would be for signal. We then compare the efficiencies for each of our companion B selection cuts in the $B^+ \rightarrow D^{(*)0}\pi^+$ data and MC simulation. Figure 2 shows a comparison of on-resonance

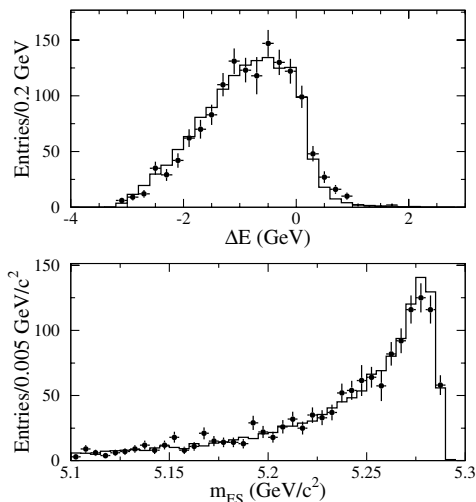


FIG. 2. The distributions of ΔE and m_{ES} of the companion B in the $B^+ \rightarrow D^0\pi^+$ control sample after all previous cuts have been applied. The points are the on-resonance data while the histogram is the MC simulation normalized to the number of reconstructed $B^+ \rightarrow D^0\pi^+$ decays. The observed discrepancies between data and simulation are accounted for by correcting the signal efficiency obtained from the simulation.

data and simulation for the ΔE and m_{ES} distributions in the $B^+ \rightarrow D^0\pi^+$ control sample. We expect the resolution observed in the control sample to represent that of $B^+ \rightarrow \mu^+\nu_\mu$ signal events. We find that the efficiency after all selection cuts in the data is a factor of 0.94 ± 0.04 times the prediction of the simulation. The signal efficiency obtained from the simulation is therefore corrected by this factor and a systematic error of 4.3% is applied. A summary of the systematic uncertainties in the signal efficiency is given in Table II. We estimate the overall signal selection efficiency to be $2.09 \pm 0.06(\text{stat}) \pm 0.13(\text{syst})\%$.

In the on-resonance data, we find 11 events in the signal box where $5.0^{+1.8}_{-1.4}$ background events are expected. The distribution of the data in the $(\Delta E, m_{\text{ES}})$ plane is shown in Fig. 3. Using a Monte Carlo technique [10], we determine the 90% C.L. upper limit on the signal to be $n_{\text{UL}} = 12.1$ events. Systematic uncertainties are included following the prescription given in Ref. [11]. The probability of a

TABLE II. Contributions to the systematic uncertainty on the signal efficiency.

Source	Correction	Uncertainty
Tracking efficiency		
Muon	0.992	2.0%
Companion B	...	1.0%
Muon identification	...	4.2%
Companion B reconstruction	0.94	4.3%
Total	0.932	6.4%

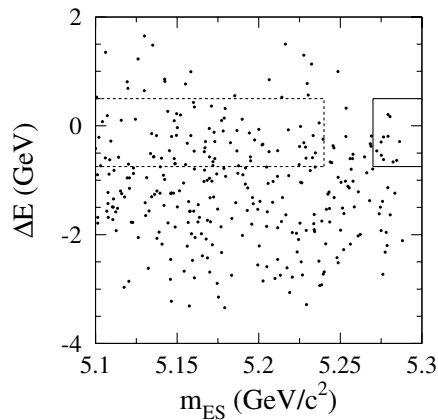


FIG. 3. The distribution of ΔE vs m_{ES} in the on-resonance data after all selection criteria have been applied. The signal box is represented by the solid lines while the dashed lines indicate the region used to estimate the background.

background fluctuation yielding the observed number of events or more is about 4%. We set an upper limit on the $B^+ \rightarrow \mu^+ \nu_\mu$ branching fraction using $\mathcal{B}(B^+ \rightarrow \mu^+ \nu_\mu) < n_{UL}/S$, where S is the product of the signal efficiency and the number of B^\pm mesons in the sample. Assuming equal production of B^0 and B^+ in $Y(4S)$ decays, the number of B^\pm mesons in the on-resonance data is estimated to be 88.4×10^6 with an uncertainty of 1.1%. We find

$$\mathcal{B}(B^+ \rightarrow \mu^+ \nu_\mu) < 6.6 \times 10^{-6}$$

at the 90% C.L. This result improves the previous best published limit for this mode by about a factor of 3 yet remains roughly an order of magnitude above the SM expectation. Despite this improved limit, the most stringent constraints on SM parameters and new physics obtainable from the $B^+ \rightarrow \ell^+ \nu_\ell$ decays are currently derived from $B^+ \rightarrow \tau^+ \nu_\tau$ searches.

We are grateful for the excellent luminosity and machine conditions provided by our PEP-II colleagues, and for the substantial dedicated effort from the computing organizations that support *BABAR*. The collaborating institutions wish to thank SLAC for its support and kind hospitality. This work is supported by DOE and NSF (U.S.A.), NSERC (Canada), IHEP (China), CEA and CNRS-IN2P3 (France), BMBF and DFG (Germany), INFN (Italy), FOM (The Netherlands), NFR (Norway), MIST (Russia), and PPARC (United Kingdom). Individuals have received support from the A. P. Sloan Foundation, Research Corporation, and Alexander von Humboldt Foundation.

*Also with Università della Basilicata, Potenza, Italy.

†Also with IFIC, Instituto de Física Corpuscular, CSIC-Universidad de Valencia, Valencia, Spain.

‡Deceased.

- [1] S. M. Ryan, Nucl. Phys. Proc. Suppl. **106**, 86 (2002).
- [2] CLEO Collaboration, M. Artuso *et al.*, Phys. Rev. Lett. **75**, 785 (1995).
- [3] L3 Collaboration, M. Acciarri *et al.*, Phys. Lett. B **396**, 327 (1997).
- [4] W. S. Hou, Phys. Rev. D **48**, 2342 (1993).
- [5] S. Baek and Y. G. Kim, Phys. Rev. D **60**, 077701 (1999).
- [6] *BABAR* Collaboration, A. Palano *et al.*, Nucl. Instrum. Methods Phys. Res., Sect. A **479**, 1 (2002).
- [7] GEANT4 Collaboration, S. Agostinelli *et al.*, Nucl. Instrum. Methods Phys. Res., Sect. A **506**, 250 (2003).
- [8] G. C. Fox and S. Wolfram, Phys. Rev. Lett. **41**, 1581 (1978).
- [9] The ARGUS function is defined by $\mathcal{A}(m_{ES}) \propto m_{ES} \sqrt{1 - m_{ES}^2/E_b^{*2}} \exp[-\zeta(1 - m_{ES}^2/E_b^{*2})]$. ARGUS Collaboration, H. Albrecht *et al.*, Phys. Lett. B **241**, 278 (1990).
- [10] R. Barlow, Comput. Phys. Commun. **149**, 97 (2002).
- [11] R. D. Cousins and V. L. Highland, Nucl. Instrum. Methods Phys. Res., Sect. A **320**, 331 (1992).